

# The use of the $\tau$ in new particle searches at DELPHI

G. Gómez-Ceballos<sup>a\*</sup>

<sup>a</sup>Instituto de Física de Cantabria (CSIC-UC), Avda. los Castros s/n, ES-39005 Santander, Spain

Several new particle searches have been performed in the DELPHI experiment involving  $\tau$  leptons in the resulting final state. The topology and special characteristics of the  $\tau$  leptons have been used to discriminate the signal from the Standard Model background. Limits on new particles have been set, playing an important role the channels with  $\tau$  leptons.

## 1. Introduction

$\tau$  leptons are not only a precision measurement tool, but also a sensitive probe for Physics beyond the Standard Model. In this note we review the importance of their contribution and the results obtained at the DELPHI experiment at LEP. Several extensions to the Standard Model predict the existence of new particles involving  $\tau$  leptons in the resulting final state.

Data collected at LEP2 at centre-of-mass energies from 130 GeV to 209 GeV were used in the different analyses, with a total integrated luminosity of about  $650 \text{ pb}^{-1}$ .

## 2. The DELPHI detector

DELPHI was one of the four detectors operating at the LEP collider from 1989 to 2000. It was designed as a general purpose detector for  $e^+e^-$  physics with special emphasis on precise tracking and vertex determination and on powerful particle identification. A detailed description of the DELPHI detector can be found in [1] and the detector and trigger performance in [2,3].

Charged particle tracks are reconstructed by a system of tracking chambers inside the 1.2 T solenoidal magnetic field: the Vertex Detector (VD), the Inner Detector (ID), the Time Projection Chamber (TPC) and the Outer Detector (OD) in the barrel region; two sets of planar drift chambers aligned perpendicular to the beam axis (Forward Chambers A and B) measure tracks in

the forward and backward directions.

The VD consists of three cylindrical layers of silicon detectors, at radii 6.3 cm, 9.0 cm and 11.0 cm, and polar angle acceptance from  $24^\circ$  to  $156^\circ$ . All three layers measure coordinates in the plane transverse to the beam ( $xy$ ), and at least two of the layers also measure  $z$  coordinates along the beam direction. The ID consists of a cylindrical drift chamber with inner radius 12 cm and outer radius 22 cm, surrounded by 5 layers of straw tubes, having a polar acceptance between  $15^\circ$  and  $165^\circ$ . The TPC, the principal tracking device of DELPHI, consists of a 2.7 m long cylinder of 30 cm inner radius and 122 cm outer radius. Each end-plate of the TPC is divided into 6 sectors with 192 sense wires and 16 circular pad rows per sector. The wires help in charged particle identification by measuring the specific energy loss ( $dE/dx$ ) and the pad rows are used for 3 dimensional space-point reconstruction. The OD consists of 5 layers of drift cells at radii between 192 cm and 208 cm, covering polar angles between  $43^\circ$  and  $137^\circ$ .

The electromagnetic calorimeters consist of a High Density Projection Chamber (HPC) covering the polar angle region from  $40^\circ$  to  $140^\circ$  and, a Forward ElectroMagnetic Calorimeter (FEMC) covering the polar angle regions from  $11^\circ$  to  $36^\circ$  and from  $144^\circ$  to  $169^\circ$ . The Scintillator Tile Calorimeter (STIC) extends the polar angle coverage down to  $1.66^\circ$  from the beam axis in both directions. The Hadron CALorimeter (HCAL) covers 98% of the solid angle. The muons which traverse the HCAL are recorded in a set of Muon

---

\*Now in the Massachusetts Institute of Technology

Drift Chambers placed in the barrel, forward and backward regions.

The Ring Imaging Cherenkov (RICH) detectors of DELPHI provide charged particle identification in both the barrel (BRICH) and forward (FRICH) regions. In addition, a set of scintillation counters were added to veto photons in blind regions of the electromagnetic calorimeter at polar angles near 40, 90 and 140 degrees.

### 3. Particle identification

An isolated particle was identified as a muon if it gave signal in the muon chambers or left a signal in the calorimeters compatible with a MIP. It was identified as an electron if its energy deposition in the electromagnetic calorimeters was compatible with its measured momentum and the ionisation loss in the TPC was compatible with that expected from an electron of that momentum.

If an electron or muon had low momentum, it was assumed to come from  $\tau$  decay and was therefore tagged as  $\tau$ . In addition isolated jets with an energy of at least 5 GeV, at least one and at most five charged tracks and no more than ten particles in total were also considered as  $\tau$  candidates.

The  $\tau$  decays were classified into the following categories:  $e$ ,  $\mu$ ,  $\pi$ ,  $\pi + n\gamma$ ,  $3\pi$  and others according to the lepton identification, the number of charged tracks of the jet and the number of photons.

### 4. Topics

Several searches with  $\tau$  leptons in the final state are reviewed. Here, we will explain briefly the  $\tau$  channels and will present the results with the combination of the rest of the possible decay channels.

#### 4.1. SM Higgs and MSSM neutral Higgs bosons

The Standard Model (SM) Higgs search has been one of the most important goals at LEP2. A scalar Higgs could be produced at LEP in the process  $e^+e^- \rightarrow HZ$ . In the Minimal Supersymmetric Standard Model (MSSM), the production of the lightest scalar Higgs boson,  $h$ , proceeds

through the same processes as in the SM. There is also a CP-odd pseudo-scalar,  $A$ , which would be produced mostly in the  $e^+e^- \rightarrow hA$  process at LEP2 [4].

The  $\text{BR}(H \rightarrow \tau^+\tau^-) \sim 5\%$ , then the  $\tau^+\tau^-q\bar{q}$  channels corresponds to  $\sim 9\%$  of the total decays. In the case of the MSSM neutral Higgs bosons the  $\tau^+\tau^-b\bar{b}$  channels corresponds to  $\sim 16\%$ . The same analysis was applied in the four channels with  $\tau$  leptons [5].

After a hadronic preselection a search for  $\tau$  lepton candidates was then performed using a likelihood ratio technique. The likelihood variable was calculated for the preselected particles using distributions of the particle momentum, of its isolation angle and of the probability that it came from the primary vertex. Pairs of  $\tau$  candidates were then selected requiring opposite charges, an opening angle greater than  $90^\circ$  and a product of the  $\tau$  likelihood variables above 0.45. If more than one pair was selected, only the pair with the highest product was kept. For the final selection another likelihood variable is built with the following variables: the rescaling factors of the  $\tau$  jets, the  $\tau$  momenta and the global  $b$ -tagging variable. Distributions of four analysis variables at different levels of the selection are shown in Fig. 1.

For all searches analyses a likelihood ratio technique [6] has been used to compute the cross-section and mass limits. No evidence of Higgs boson production was found neither in the SM Higgs search nor the MSSM neutral Higgs search. The distribution of the sum of the reconstructed Higgs boson masses for the tight candidates in each channel from the 2000 data in the SM Higgs search is shown in Fig. 2. With combination of all channels the lower limit at 95% CL was set on the mass of the Standard Model Higgs boson at:

$$m_H > 114.1 \text{ GeV}/c^2$$

The following limits are derived in the framework of the MSSM:

$$m_h > 89.1 \text{ GeV}/c^2 \text{ and } m_A > 90.0 \text{ GeV}/c^2$$

for all values of  $\tan\beta$  above 0.44 and assuming the mixing in the stop sector.

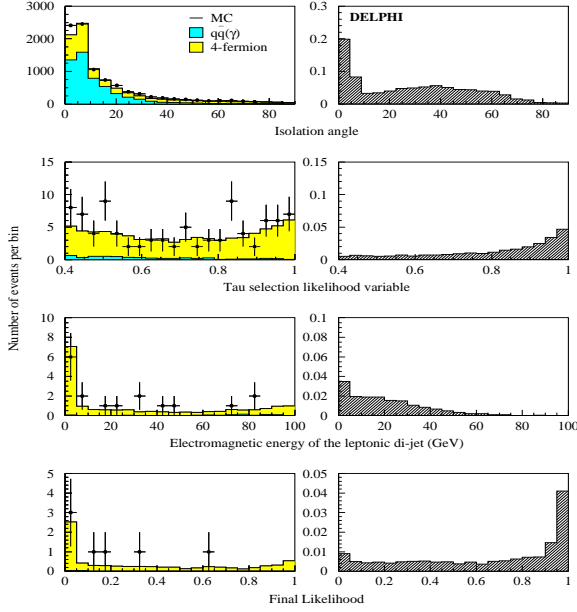


Figure 1. Distributions of four analysis variables at different levels of the selection in the  $\tau^+\tau^-q\bar{q}$  channel in the search for neutral Higgs bosons. Data from  $\sqrt{s}=202\text{-}209$  GeV (dots) are compared with SM background process expectations (left-hand side histograms). The expected distribution for a  $115$  GeV/ $c^2$  Higgs signal in the ( $hZ \rightarrow \tau^+\tau^-q\bar{q}$ ) channel is shown in the right-hand side plots.

#### 4.2. Charged Higgs bosons 2HDM type II

The existence of a pair of charged Higgs bosons is predicted by several extensions of the Standard Model. Pair-production of charged Higgs bosons occurs mainly via  $s$ -channel exchange of a photon or a  $Z^0$  boson. In two Higgs doublet models (2HDM), the couplings are completely specified in terms of the electric charge and the weak mixing angle,  $\theta_W$ , and therefore the production cross-section depends only on the charged Higgs boson mass. Higgs bosons couples to mass and therefore decay preferentially to heavy particles, but the precise branching ratios may vary significantly depending on the model. In 2HDM type II, where

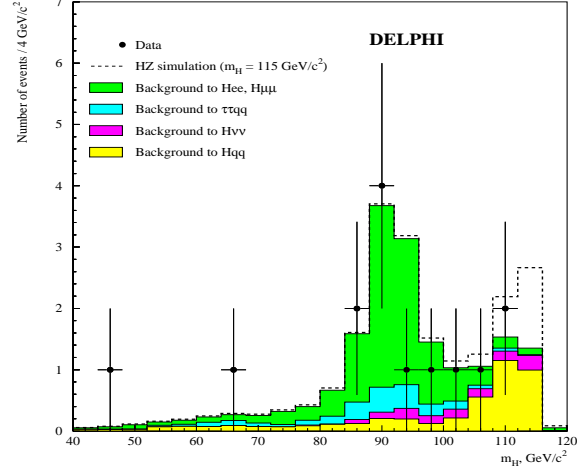


Figure 2. Distribution of the sum of the reconstructed Higgs boson masses for the tight candidates in each channel from the 2000 data in the SM Higgs search.

the down/up fermions couple to  $H_1/H_2$  Higgs fields respectively, the  $\tau\nu_\tau$  and  $cs$  decay channels are expected to dominate. There are two channels with  $\tau$  leptons in the final state: the purely leptonic channel ( $H^+H^- \rightarrow \tau^+\nu_\tau\tau^-\bar{\nu}_\tau$ ) and the semileptonic channels ( $H^+H^- \rightarrow qq'\tau\nu$ ) [7].

In both cases the main remaining background coming from  $W$ -pair production. Apart from the reconstructed mass, which is not possible to reconstruct in the leptonic channel, there are two important difference to discriminate both contributions: the  $\tau$  polarization and the boson production polar angle.

- $\tau$  polarization:

assuming that the  $\nu_\tau$  has a definite helicity, the polarization ( $P_\tau$ ) of tau leptons originating from heavy boson decays is determined entirely by the properties of weak interactions and the nature of the parent boson. The helicity configuration for the signal is  $H^- \rightarrow \tau_R^- \bar{\nu}_{\tau R}$  ( $H^+ \rightarrow \tau_L^+ \nu_{\tau L}$ ) and for the  $W^+W^-$  background it is  $W^- \rightarrow \tau_L^- \bar{\nu}_{\tau R}$  ( $W^+ \rightarrow \tau_R^+ \nu_{\tau L}$ ) resulting in  $P_\tau^H = +1$  and

$P_\tau^W = -1$ . The  $\tau$  weak decay induces a dependence of the angular and momentum distributions on polarization. Once the  $\tau$  decay channel is identified, the information on the  $\tau$  polarization was extracted from the observed kinematic distributions of its decay products, e.g. angles and momenta. These estimators are equivalent to those used at the Z peak for precision measurements [8]. For charged Higgs boson masses close to the threshold, the boost of the bosons is relatively small and the  $\tau$  energies are similar to the  $\tau$ 's from Z decays at rest (40–50 GeV).

- Boson production polar angle:

$H$ -pair production occurs via s-channel and the differential cross-section follows a behavior proportional to  $1 + \cos^2\theta$ . But,  $W$ -pair production occurs via s-channel and t-channel. Then, the  $W$  production polar angle distribution goes to  $\cos\theta_W \sim 1$ , and the  $W^-$  ( $W^+$ ) is emitted preferentially in the direction of  $e^-$  ( $e^+$ ).

In the leptonic channel, the selection is performed in similar way to the  $W^+W^- \rightarrow \tau^+\nu_\tau\tau^-\bar{\nu}_\tau$  [9]. After that selection, a likelihood to separate the signal from the background was built using six variables: the estimators of the  $\tau$  polarization, the boson polar angle of both  $\tau$  leptons, the acoplanarity and the total transverse momentum. These variables are shown in Fig. 3.

In the semileptonic channel two likelihood variables were built to reject the  $QCD$  background and the  $WW$  background. In the anti- $WW$  likelihood the estimator of the  $\tau$  polarization and the reconstructed polar angle of the negatively boson are included.

No significant signal-like excess of events compared to the expected backgrounds was observed in any of the three final states investigated. A lower limit for a charged Higgs boson mass was set at 95% confidence level of  $M_{H^\pm} > 74.3$  GeV/ $c^2$ , assuming  $\text{BR}(H \rightarrow \tau\nu) + \text{BR}(H \rightarrow cs) = 1$ . The observed and expected exclusion regions at 95% confidence level in the plane of  $\text{BR}(H \rightarrow \tau\nu_\tau)$  vs.  $M_{H^\pm}$  are shown in Fig. 4. The noticeable

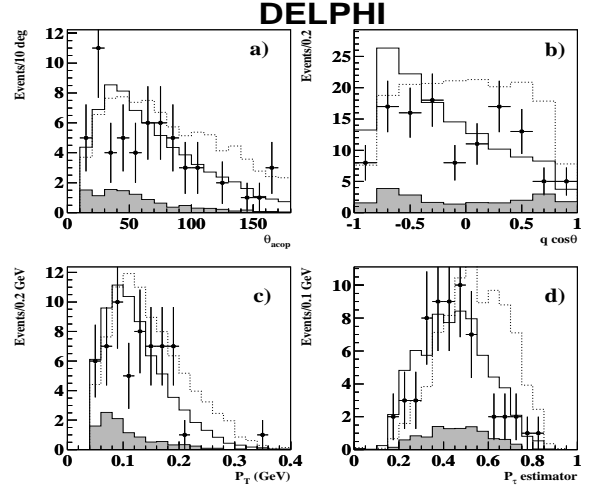


Figure 3. Distribution of the variables used for the anti- $WW$  likelihood for the  $\tau\nu\tau\nu$  analysis after preselection: a) acoplanarity, b) cosine of polar angle accounting for the charge, c) transverse momentum scaled by the center-of-mass energy and d)  $\tau$  polarization estimator. Data are shown as filled circles, while the solid histogram contour shows the expected SM background with contributions from  $WW$  (unfilled) and other contributions (shaded). The expected histogram for a 85 GeV/ $c^2$  charged Higgs boson signal is shown as a dashed line in arbitrary normalization for comparison.

difference between observed and expected limit is dominated by a small “hole” around  $\text{BR}(H \rightarrow \tau\nu)=0.35$  which reaches only 92% as confidence level, produced by a small excess of data in that region in the semileptonic channel.

#### 4.3. Charged Higgs bosons 2HDM type I

In 2HDM type I models, where all fermions couple to the same Higgs doublet, the  $H^- \rightarrow W^*A$  decay can be dominant, if the neutral pseudoscalar  $A$  is light and if  $\tan\beta$  is large enough [10]. To cover this eventuality the final states  $W^*AW^*A$  and  $W^*A\tau\nu$  were also looked

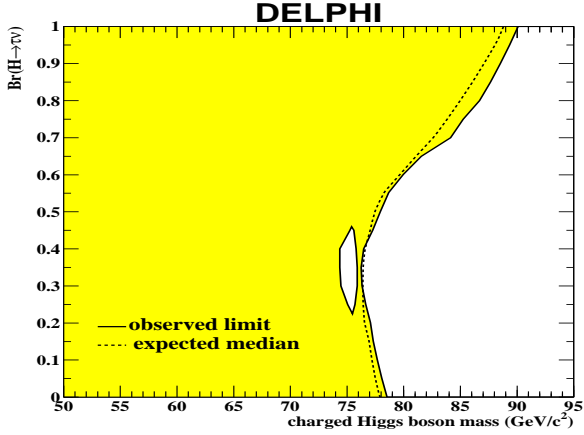


Figure 4. The observed and expected exclusion regions at 95% confidence level in the plane of  $\text{BR}(H \rightarrow \tau\nu_\tau)$  vs.  $M_{H^\pm}$ . These limits were obtained from a combination of the search results in the  $\tau\nu\tau\nu$ ,  $c s \tau\nu$  and  $c s c s$  channels at  $\sqrt{s} = 183\text{--}209$  GeV, under the assumption that the  $W^*A$  decay is forbidden.

for [7].

If at least one of the Higgs bosons decays to a  $W^*A$  pair, there are several possible topologies depending on the different boson decays. The  $W$  boson can decay leptonically or hadronically, and the number of jets strongly depends on the  $A$  mass and on the boson boosts. To treat all these decays in a generic way, the search was restricted to  $A$  masses above 12 GeV, where it decays predominantly to  $b\bar{b}$  and an inclusive search is performed. Events with jets with  $b$  quark content were searched for in two topologies: events with a  $\tau$ , missing energy and at least two hadronic jets; and events with no missing energy and at least four hadronic jets. It was found that the analysis designed by DELPHI for technicolor search[11] was well suited also for these topologies and had a good performance on this search. It was therefore adopted here. In both topologies good agreement between the data and the Standard Model expectation was found.

Therefore, with the combination of the five channels, if the  $W^*A$  decay is allowed, a lower  $H^\pm$  mass limit of  $M_{H^\pm} > 76.7$  GeV/ $c^2$  can be set at the 95% confidence level, independently of  $\tan\beta$  for  $M_A > 12$ . The observed and expected exclusion regions at 95% confidence level in the plane of  $\tan\beta$  vs.  $M_{H^\pm}$ , for different  $A$  masses, are shown in Fig. 5.

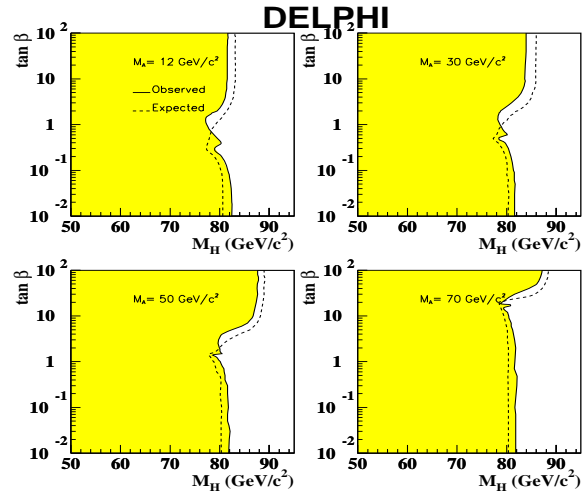


Figure 5. The observed and expected exclusion regions at 95% confidence level in the plane of  $\tan\beta$  vs.  $M_{H^\pm}$ . These limits were obtained from a combination of the search results in all five channels at  $\sqrt{s} = 183\text{--}209$  GeV, for different  $A$  masses.

#### 4.4. Technicolor search

The technicolor model [12] provides an alternative to the SM mechanism of Electroweak Symmetry breaking. Role of Higgs boson is performed by bound states of new fundamental fermions, Techniquarks, which mix with  $W$  and  $Z$ , and generate their masses. These bosons are seen as condensates of a new family of quarks (the techniquarks) which obey a QCD-like interaction with an effec-

tive scale  $\Lambda_{TC}$  much larger than  $\Lambda_{QCD}$ . It also predicts heavy ( $> 1$  TeV) vector mesons which cannot be observed at LEP2.

The main  $\rho_T$  decay modes are  $\rho_T \rightarrow \pi_T \pi_T$ ,  $W_L \pi_T$ ,  $W_L W_L$ ,  $f_i \bar{f}_i$  and  $\pi_T^0 \gamma$ , where  $W_L$  is the longitudinal component of the  $W$  boson. For  $M_{\rho_T} > 2M_{\pi_T}$  the decay  $\rho_T \rightarrow \pi_T \pi_T$  is dominant, while for  $M_{\rho_T} < 2M_{\pi_T}$  the decay rates depend on many model parameters. Technipions can also be produced at LEP through virtual  $\rho_T$  exchange. Technipions are assumed to decay as  $\pi_T^+ \rightarrow c\bar{b}$ ,  $c\bar{s}$  and  $\tau^+ \nu_\tau$ ; and  $\pi_T^0 \rightarrow b\bar{b}$ ,  $c\bar{c}$  and  $\tau^+ \tau^-$ . The width  $\Gamma(\pi_T \rightarrow f' f)$  is proportional to  $(m_f + m_{f'})^2$ , therefore the  $b$ -quark is produced in  $\sim 90\%$  of  $\pi_T$  decays. The total  $\pi_T$  width is less than 1 GeV. The analyses performed by DELPHI use the off-shell processes  $e^+ e^- \rightarrow \rho_T^* \rightarrow (\pi_T^+ \pi_T^-, \pi_T^+ W_L^-)$  and  $e^+ e^- \rightarrow (\rho_T^*, \omega_T^*) \rightarrow \pi_T^0 \gamma$ .

The search for the technipion [11] in semileptonic channels containing two quarks, a lepton and a neutrino, corresponds to the decays  $W_L^+ \pi_T^- \rightarrow l^+ \nu_l b \bar{c}$  and  $\pi_T^+ \pi_T^- \rightarrow \tau^- \bar{\nu}_\tau b \bar{c}$ . The first step in the analysis was a  $qq'l\nu$  selection. The second step exploits the specific properties of the signal, such as the presence of  $b$ -quarks or the production angle, to distinguish it from the  $W$  pairs. This is done building a neural network which uses four input variables: the  $b$ -tagging variables of the two hadronic jets,  $\cos \theta_{W^-}$  and  $|\cos \theta_{miss}|$ .

Good agreement between the data and the SM background was observed in all channels studied in this search. The combined region in the  $(M_{\rho_T}, M_{\pi_T})$  plane excluded by this analysis at a 95% CL is shown for  $N_D = 2$  (maximal  $W_L - \pi_T$  mixing) in Figure 6.

#### 4.5. Invisibly decaying Higgs bosons

Some extensions of the SM exhibit Higgs bosons which can decay into stable neutral weakly interacting particles, therefore giving rise to invisible final states. In supersymmetric models the Higgs bosons can decay with a large branching ratio into lightest neutralinos or gravitinos in some region of the parameter space, leading to an invisible final state if  $R$  parity<sup>2</sup> is conserved [13–16].

<sup>2</sup>R-parity is a multiplicative quantum number defined as  $R_P = (-1)^{3B+L+2S}$  where  $B$ ,  $L$  and  $S$  are the baryon number, the lepton number and the spin of the particle,

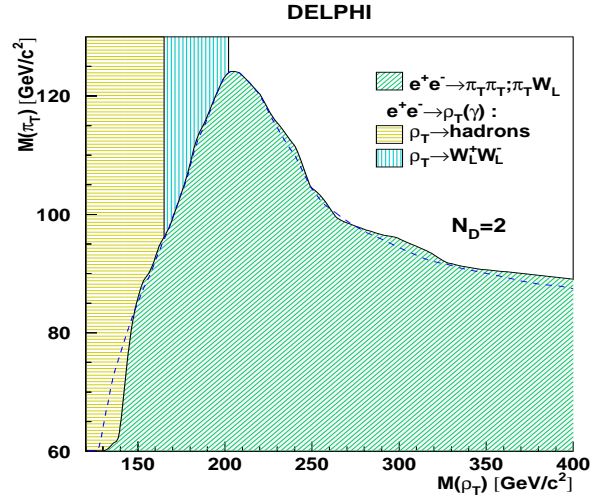


Figure 6. The region in the  $(M_{\rho_T} - M_{\pi_T})$  plane (filled area) excluded at 95% CL for  $N_D = 2$  (maximal  $W_L - \pi_T$  mixing). The dashed line shows the expected limit for the  $e^+ e^- \rightarrow \pi_T \pi_T, \pi_T W_L$  search.

Searches for HZ production with the Higgs boson decaying into an invisible final state were performed by the DELPHI experiment. Both hadronic and leptonic final states of the  $Z$  boson were analyzed. DELPHI has been analyzed the four possible visible final states channels, including the  $\tau^+ \tau^-$  channel.

The selection is explained in detail in [17], and it was performed in similar way as other searches with two  $\tau$  leptons plus additional non-interacting particles. The mass of the invisibly decaying particle was computed from the measured energies assuming momentum and energy conservation. In the case of the  $\tau^+ \tau^-$  channel, the information carried by the decay products does not reproduce correctly the  $\tau$  energy. Therefore, the mass is calculated under the assumption that both  $\tau$  leptons had the same energy.

respectively. SM particles have  $R = +1$ , while their SUSY particles have  $R = -1$ .

From the comparison with the SM Higgs boson cross-section, and combining the four final states investigated, the observed (expected) mass limits are 112.1 (110.5)  $\text{GeV}/c^2$  for the Higgs boson decaying into invisible particles. The excluded regions in the MSSM from searches for Higgs boson decaying into invisible final states for  $m_h$ -max in the stop sector are shown in Fig. 7.

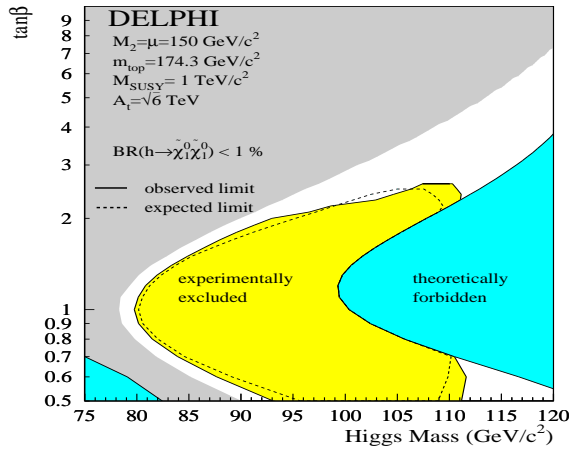


Figure 7. Excluded region in the MSSM from searches for Higgs boson decaying into invisible final states for  $m_h$ -max in the stop sector. The different grey areas show the theoretically forbidden region (dark), the region where the Higgs boson does not decay into neutralinos (intermediate), the region which is excluded at 95% CL by this search for invisibly decaying Higgs bosons (light) and the unexcluded region (white).

#### 4.6. SUSY searches

Supersymmetry (SUSY) is at present one of the most attractive possible extensions of the SM and its signatures could be observed at LEP through a large variety of different channels [18]. Supersymmetry (SUSY) is usually assumed to be broken in a hidden sector of particles and then communicated to the observable sector (where all the

particles and their superpartners lie) via gravitational interactions. But there are other possibilities where this mediation is performed by SM gauge interactions, leading to models of gauge mediated supersymmetry breaking.

Many channels and several scenarios have been studied with  $\tau$  leptons in the final state. DELPHI have performed searches for supersymmetric particles within the framework of the MSSM assuming R-parity conservation [19] (implying that the Lightest Supersymmetric Particle, LSP, is stable and SUSY particles are pair-produced), with R-parity violation [20], in Gauge Mediated Supersymmetry Breaking (GMSB) models [21] and in Anomaly Mediated SUSY Breaking (AMSB) models [22].

As an example, the different topologies studied in the GMSB framework are summarized in Table 1. The  $\tau$  leptons appear in several channels: acoplanar leptons (2 leptons + missing energy), kinks and large impact parameters (when the sparticle decays inside the detector) and four leptons + missing energy (if  $\tilde{\tau}$  is the Next Lightest Supersymmetric Particle, then there are  $4\tau$  in the final state).

Production	Decay mode	$\tilde{L}$
$\tilde{l}\bar{l}$	$\tilde{l} \rightarrow l\tilde{G}$	$\ll l_{detector}$ $\sim l_{detector}$ $\gg l_{detector}$
$\tilde{\chi}_1^0\tilde{\chi}_1^0$	$\tilde{\chi}_1^0 \rightarrow \tilde{l}l \rightarrow ll\tilde{G}$	$\ll l_{detector}$
$\tilde{\chi}_1^+\tilde{\chi}_1^-$	$\tilde{\chi}_1^+ \rightarrow \tilde{l}^+\nu \rightarrow l^+\tilde{G}\nu$	$\ll l_{detector}$ $\sim l_{detector}$ $\gg l_{detector}$
$\phi\gamma$	$\phi \rightarrow \gamma\gamma$ $\phi \rightarrow gg$	$\ll l_{detector}$ $\ll l_{detector}$

Table 1

Final state topologies studied in the different scenarios, within the GMSB models.

In all cases no evidence for signal production was found. Hence, the DELPHI collaboration set lower limit at 95% C.L. for the sparticle masses. Exclusion regions in the  $(m_{\tilde{G}}, m_{\tilde{\tau}_1})$  plane

at 95% CL combining all analyses in GMSB models are shown in Fig. 8.

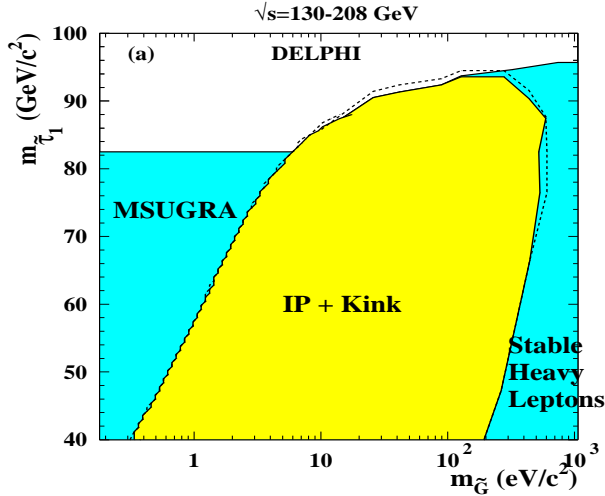


Figure 8. Exclusion regions in the  $(m_{\tilde{G}}, m_{\tau_1})$  plane at 95% CL combining all analyses in GMSB models.

#### 4.7. Doubly charged Higgs bosons

Doubly charged Higgs bosons ( $H^{\pm\pm}$ ) appear in several extensions to the Standard Model [23], such as left-right symmetric models, and can be relatively light. In Supersymmetric left-right models usually the  $SU(2)_R$  gauge symmetry is broken by two triplet Higgs fields, so-called left and right handed. Pair-production of doubly charged Higgs bosons is expected to occur mainly via  $s$ -channel exchange of a photon or a Z boson. In left-right symmetric models the cross-section of  $e^+e^- \rightarrow H_L^{++}H_L^{--}$  is different from that for  $e^+e^- \rightarrow H_R^{++}H_R^{--}$ , where  $H_L^{\pm\pm}$  and  $H_R^{\pm\pm}$  are the left-handed and right-handed Higgs bosons.

The dominant decay mode of the doubly charged Higgs boson is expected to be a same sign charged lepton pair, the decay proceeding via a lepton number violating coupling. As discussed

in [24], due to limits that exist for the couplings of  $H^{\pm\pm} \rightarrow e^\pm e^\pm$  from high energy Bhabha scattering,  $H^{\pm\pm} \rightarrow \mu^\pm \mu^\pm$  from the absence of muonium to anti-muonium transitions and  $H^{\pm\pm} \rightarrow \mu^\pm e^\pm$  from limits on the flavour changing decay  $\mu^\pm \rightarrow e^\mp e^\pm e^\pm$ , electron and muon decays are not likely. In addition, most of the models expect that the coupling to  $\tau\tau$  will be much larger than any of the others. Therefore, only the doubly charged Higgs boson decay  $H^{\pm\pm} \rightarrow \tau^\pm \tau^\pm$  is considered by DELPHI [25].

Depending on the  $h_{\tau\tau}$  coupling and the Higgs mass the experimental signature is different. If  $h_{\tau\tau}$  is sufficiently large,  $h_{\tau\tau} \geq 10^{-7}$ , the Higgs decays very close to the interaction point. If  $h_{\tau\tau}$  is smaller the decay occurs inside the tracking detectors (the analysis used in the search for kinks in GSMB models is adopted here) or even beyond them (search for stable massive particles). In the first case, the resulting final state consists of four narrow and low multiplicity  $\tau$  jets coming from the interaction point. The analysis was performed in several steps: first a four jet pre-selection was applied, followed by some cuts to reject the 2-photon and the 4-lepton background. Finally the mass was built requiring energy and momentum conservation. After all requirements were applied only one event was observed in the data, while 0.9 events were expected from background processes.

The three different analyses were applied to cover the whole range of the  $h_{\tau\tau}$  coupling, and good agreement between the data and the SM background was observed. Fig. 9 shows the 95% confidence level upper limits on the cross-section at  $\sqrt{s} = 206.7$  GeV for the production of  $H^{++}H^{--} \rightarrow \tau^+\tau^+\tau^-\tau^-$  for different values of  $h_{\tau\tau}$ . The comparison of these limits with the expected cross-section for left-handed  $H_L^{\pm\pm}$  and right-handed  $H_R^{\pm\pm}$  pair production yields 95% confidence level lower limits for any value of the  $h_{\tau\tau}$  coupling on the mass of the  $H_L^{\pm\pm}$  and  $H_R^{\pm\pm}$  bosons of 98.1 and 97.3 GeV/c<sup>2</sup> respectively.

#### 4.8. Searches for Neutral Higgs Bosons in Extended Models

The simplest extensions of the Standard Model are the so-called Two-Higgs Doublet Models



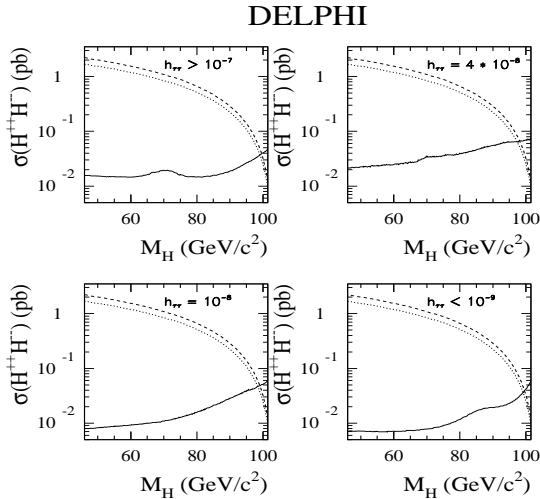


Figure 9. The solid line shows the 95% confidence level upper limit on the  $H^{\pm\pm}$  pair production cross-section at  $\sqrt{s}=206.7$  GeV assuming 100% branching ratio for the decay of  $H^{\pm\pm}$  into  $\tau^{\pm}\tau^{\pm}$  for different values of  $h_{\tau\tau}$ . The dashed and dotted lines show the expected production cross-section of  $H_L^{\pm\pm}$  and  $H_R^{\pm\pm}$  pairs in left-right symmetric models.

(2HDM), of which various types exist, depending on the choice of the scalar couplings to fermions [4]. The first type assumes that one doublet only couples to fermions while the other one couples to gauge bosons. The resulting final states display Higgs boson decays into photon pairs. The second and most studied type assumes that one doublet couples to the up-type fermions (neutrinos and the u,c,t quarks) while the other one couples to down-type fermions (charged leptons and the d,s and b quarks). Depending on the mixing of the two doublets, the dominant Higgs boson decays will be either c-quarks and/or gluons, or b-quarks and  $\tau$ -leptons.

Finally a third possible choice of couplings, in which one Higgs doublet couples to leptons only, while the other couples to quarks. In this unexplored case, the dominant Higgs boson decay

modes may be leptonic, leading, in the case of Higgs boson pair production, to the striking  $4\tau$  final state. For the first time at LEP2 a search for  $hA \rightarrow \tau^+\tau^-\tau^+\tau^-$  was performed at DELPHI [26]. When the Higgs mass was lower than  $\sim 25$  GeV/ $c^2$  the  $\tau$  pairs of the Higgs decay were observed as only one jet due to the low angle between both  $\tau$  leptons. Then, three different analyses were applied to keep the efficiency in a wide range of masses: '4-jet analysis', '3-jet analysis' and '2-jet analysis'.

Good agreement between the data and the expected background was observed for the combined sample, and the combination of the three independent analyses. At the final selection level, 13 events were selected in the data and 17.9 events were expected from the Standard Model background. Very strong constraints on the  $\tau$  coupling have been set with this analysis.

## 5. Conclusions

$\tau$  leptons are a sensitive probe for Physics beyond the Standard Model. A lot of new particle searches have been performed in the DELPHI experiment involving  $\tau$  leptons in the resulting final state. New techniques have been used to discriminate the signal and the background.

Good agreement between the data and the Standard Model prediction has been found in all of cases. Therefore, limits on new particles have been set, playing an important role the channels with  $\tau$  leptons.

## REFERENCES

1. DELPHI Collaboration, P. Aarnio *et al.*, Nucl. Instr. and Meth. **303** (1991) 233.
2. DELPHI Collaboration, P. Abreu *et al.*, Nucl. Instr. and Meth. **378** (1996) 57.
3. The DELPHI Trigger Group, A. Augustinus *et al.*, *The DELPHI Trigger System at LEP2* (to be submitted to Nucl.Instr.and.Meth. A).
4. J. F. Gunion, H. E. Haber, G. Kane, S. Dawson, *The Higgs Hunter's Guide*, Addison-Wesley Publishing Company.
5. Final results on SM and MSSM Neutral Higgs

- bosons (DELPHI Collaboration), paper in preparation.
6. A.L. Read, in CERN report 2000-005, p. 81
  7. Search for Charged Higgs Bosons at LEP in general two higgs doublet models (DELPHI Collaboration), paper in preparation.
  8. P. Abreu *et al.* (DELPHI Collaboration), *Zeit. Phys. C* **67** (1995) 183.
  9. P. Abreu *et al.* (DELPHI Collaboration), *Phys. Lett. B* **479** (2000) 89.
  10. A.G. Akeroyd *et al.* *Eur. Phys. J. C* **20** (2001) 51.
  11. P. Abreu *et al.* (DELPHI Collaboration), *Eur. Phys. J. C* **22** (2001) 17.
  12. For a recent review see K.Lane, *Technicolor 2000*, preprint BUHEP-00-15 (Boston U.), e-Print Archive: hep-ph/0007304, and references therein;  
See the discussion in T. Barklow *et al.* *Strong Coupling Electroweak Symmetry Breaking*, preprint SLAC-PUB-7397 (Snowmass 1996), e-Print Archive: hep-ph/9704217 and references therein;  
K.Lane, *Phys. Rev. D* **60** (1999) 075007, e-Print Archive: hep-ph/9903369;  
K.Lane, preprint BUHEP-99-5 (1999), e-Print Archive: hep-ph/9903372.
  13. A. Djouadi, P. Janot, J. Kalinowski and P.M. Zerwas, *Phys. Lett. B* **376** (1996) 220.
  14. Y. Chikashige, R.N. Mohapatra, R.D. Peccei, *Phys. Lett. B* **98** (1981) 265;  
R.E. Shrock, M. Suzuki, *Phys. Lett. B* **110** (1982) 250;  
R. Mohapatra, J.W.F. Valle, *Phys. Rev. D* **34** (1986) 1642;  
M.C. Gonzalez-Garcia, J.W.F. Valle, *Phys. Lett. B* **216** (1989) 360;  
E.D Carlson, L.J. Hall, *Phys. Rev. D* **40** (1989) 3187;  
L.F. Li, Y. Liu, L. Wolfenstein, *Phys. Lett. B* **159** (1985) 45;  
A. Zee, *Phys. Lett. B* **93** (1980) 389.
  15. F. de Campos *et al.*, *Phys. Rev. D* **55** (1997) 1316.
  16. S.P. Martin and J.D. Wells, *Phys. Rev. D* **60** (1999) 035006.
  17. Searches for invisibly decaying Higgs bosons (DELPHI Collaboration), paper in preparation.
  18. P. Fayet and S. Ferrara, *Phys. Rep.* **32** (77) 249;  
H. P. Nilles, *Phys. Rep.* **110** (84) 1;  
H. E. Haber and G. L. Kane, *Phys. Rep.* **117** (85) 75;  
P. Fayet *Phys. Lett. B* **69** (1977) 489;  
G. Farrar and P. Fayet, *Phys. Lett. B* **76** (1978) 575;  
S. Dimopoulos, S. Thomas, J.D. Wells, *Nucl. Phys. B* **488** (1997) 39;  
S. Ambrosanio, G.D. Kribs, S.P. Martin, *Phys. Rev. D* **56** (1997) 1761;  
G.F. Giudice, R. Rattazzi, *Phys. Rep.* **322** (99) 419 and *Phys. Rep.* **322** (99) 501.
  19. Searches for supersymmetric particles in e+e- collisions up to 208 GeV, and interpretation of the results within the MSSM (DELPHI Collaboration), paper in preparation.
  20. Search for Spontaneous R -parity Violation with the DELPHI detector at LEP (DELPHI Collaboration), paper in preparation;  
Search for supersymmetry with R-parity violation at  $\sqrt{s}=192$  to 208 GeV (DELPHI Collaboration), paper in preparation.
  21. Search for supersymmetric particles in light gravitino scenarios (DELPHI Collaboration), paper in preparation.
  22. Search for AMSB with the DELPHI data (DELPHI Collaboration), paper in preparation.
  23. J.F. Gunion, H.E. Haber, G.L. Kane and D. Dawson, *The Higgs Hunter's Guide*, *Frontiers in Physics, Lecture Notes Series*, Addison Wesley, 1990;  
C. S. Aulakh, A. Melfo and G. Senjanovic, *Phys. Rev. D* **57** (1998) 4174;  
Z. Chacko and R. N. Mohapatra, *Phys. Rev. D* **58** (1998) 15003.
  24. M. L. Swartz, *Phys. Rev. D* **40** (1989) 1521;  
K. Huitu *et al.*, *Nucl. Phys.*, **B487** (1997) 27.
  25. Search for doubly charged Higgs bosons at LEP2 (DELPHI Collaboration), paper in preparation.
  26. Searches for Neutral Higgs Bosons in Extended Models, the DELPHI Higgs research line, contributed paper for ICHEP 2002 (Amsterdam).